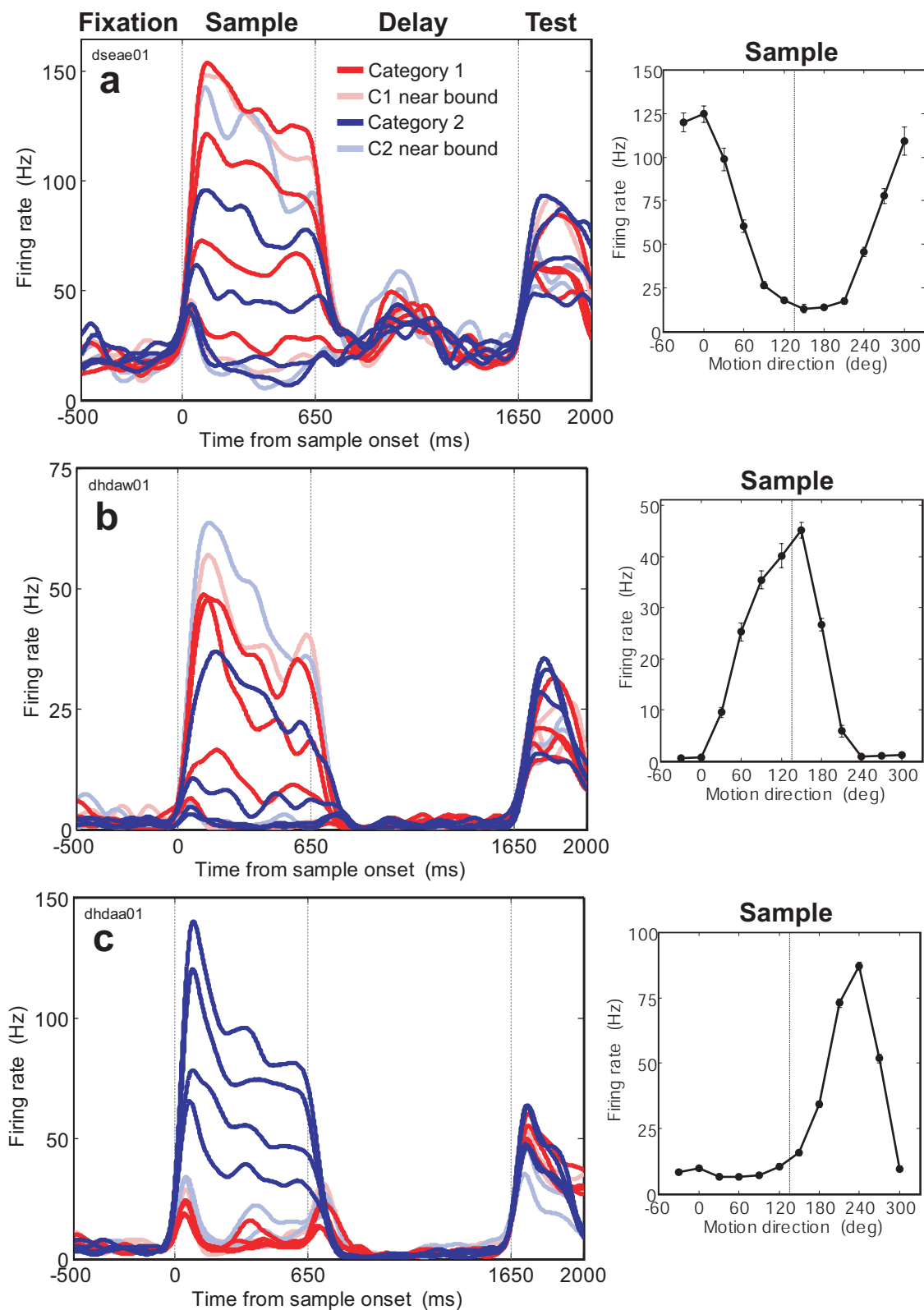
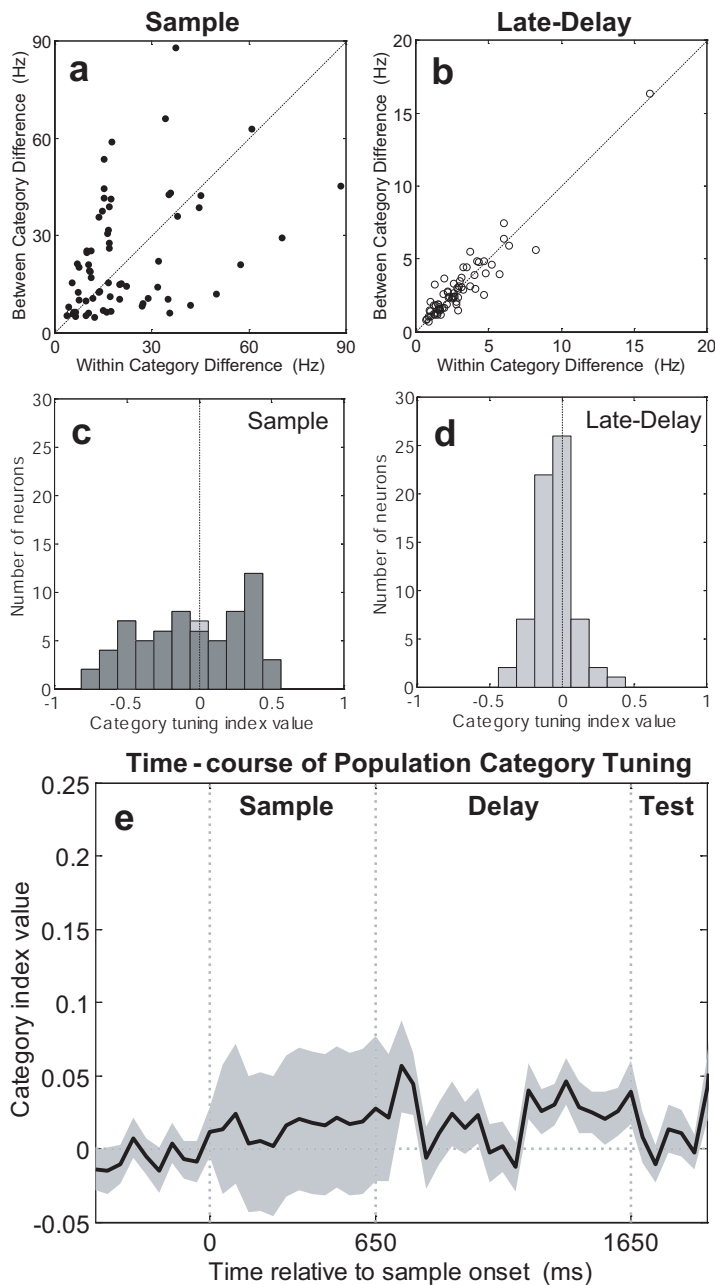


Supplementary Figure 1



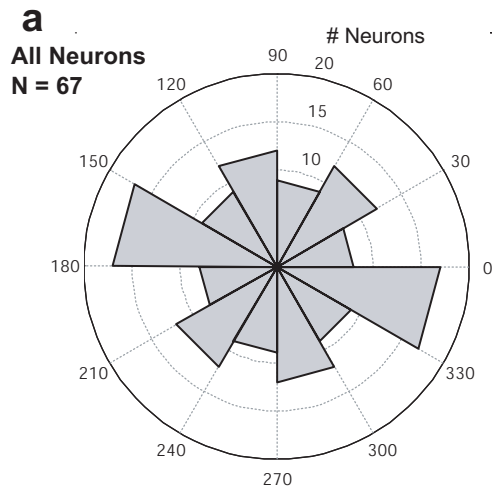
Supplementary Figure 1. Examples of three direction-selective MT neurons. Peri-stimulus time histograms (PSTH) in figures a-c show the average activity to the 12 sample stimulus directions for three single MT neurons. The red and blue colored traces indicate the directions in the two categories. The pale red and blue traces indicate those directions that were close to (15°) the category boundary. The three vertical dotted lines indicate (from left to right) the timing of sample onset, sample offset and test-stimulus onset. The plots at the right of each PSTH show the average firing rate to the 12 directions during the sample epoch. Error bars indicate the standard error of the mean.

Supplementary Figure 2

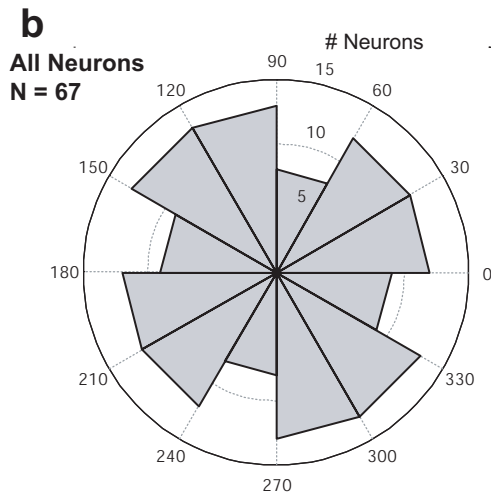


Supplementary Figure 2. Category effects across the MT population were much weaker than LIP. (a, b) Average firing rate differences for pairs of motion directions within and between categories were computed across a range of direction intervals. From these values, a between-category-difference (BCD) and within-category-difference (WCD) was computed for each neuron by averaging the between- and within-category firing rate differences, respectively (see *Methods*). BCD and WCD values are shown for the sample (a) and late-delay (b) epochs. The filled circles indicate direction-selective neurons (according to one-way ANOVA at $P < 0.01$), while the open circles correspond to non-selective neurons. **(c, d)** A category tuning index, which measured the strength of category selectivity, was computed from the BCD and WCD values (see *Methods*). Positive values of the index indicate larger activity differences between categories and more similar activity within categories. The distribution of category tuning index values is shown across the entire MT population ($N = 67$) in the sample (figure c) and late-delay (figure d). The dark grey bars indicate neurons that were direction selective. The light colored bars correspond to non-direction-selective neurons. **(e)** The time-course of category selectivity is shown by computing a “sliding” version of the category-tuning index (window width = 100 ms, step size = 50 ms) across the entire MT population ($N = 67$). The grey area around the solid black line (the mean index value) indicates the standard error of the mean.

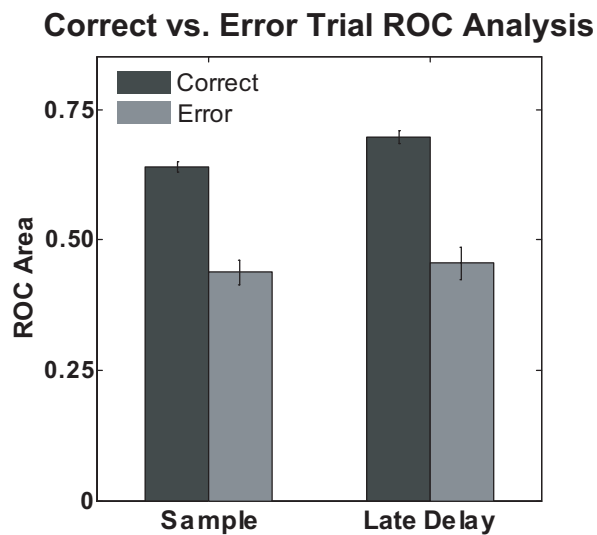
MT Category Boundary Selectivity (Sample)



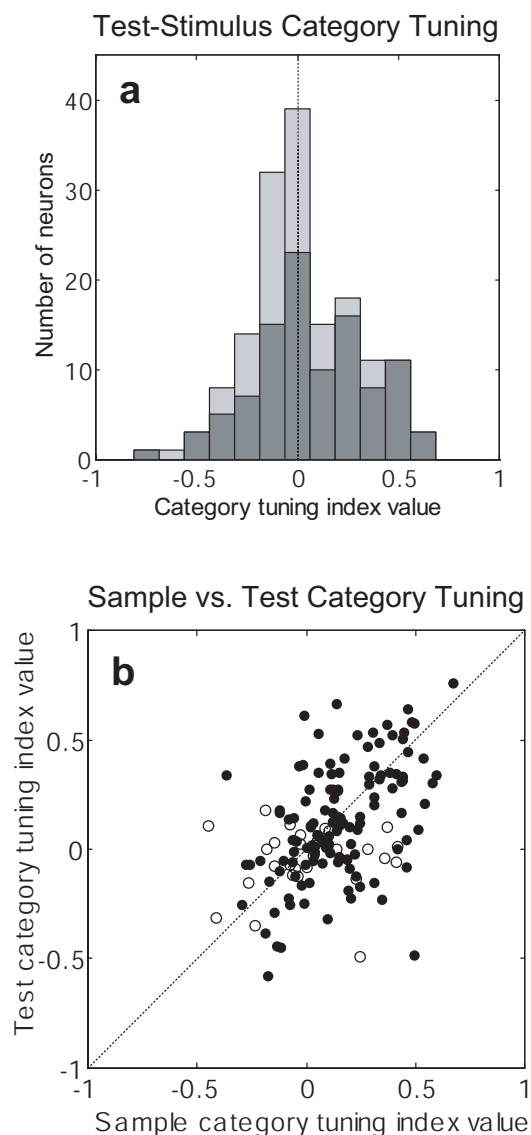
MT Category Boundary Selectivity (Late Delay)



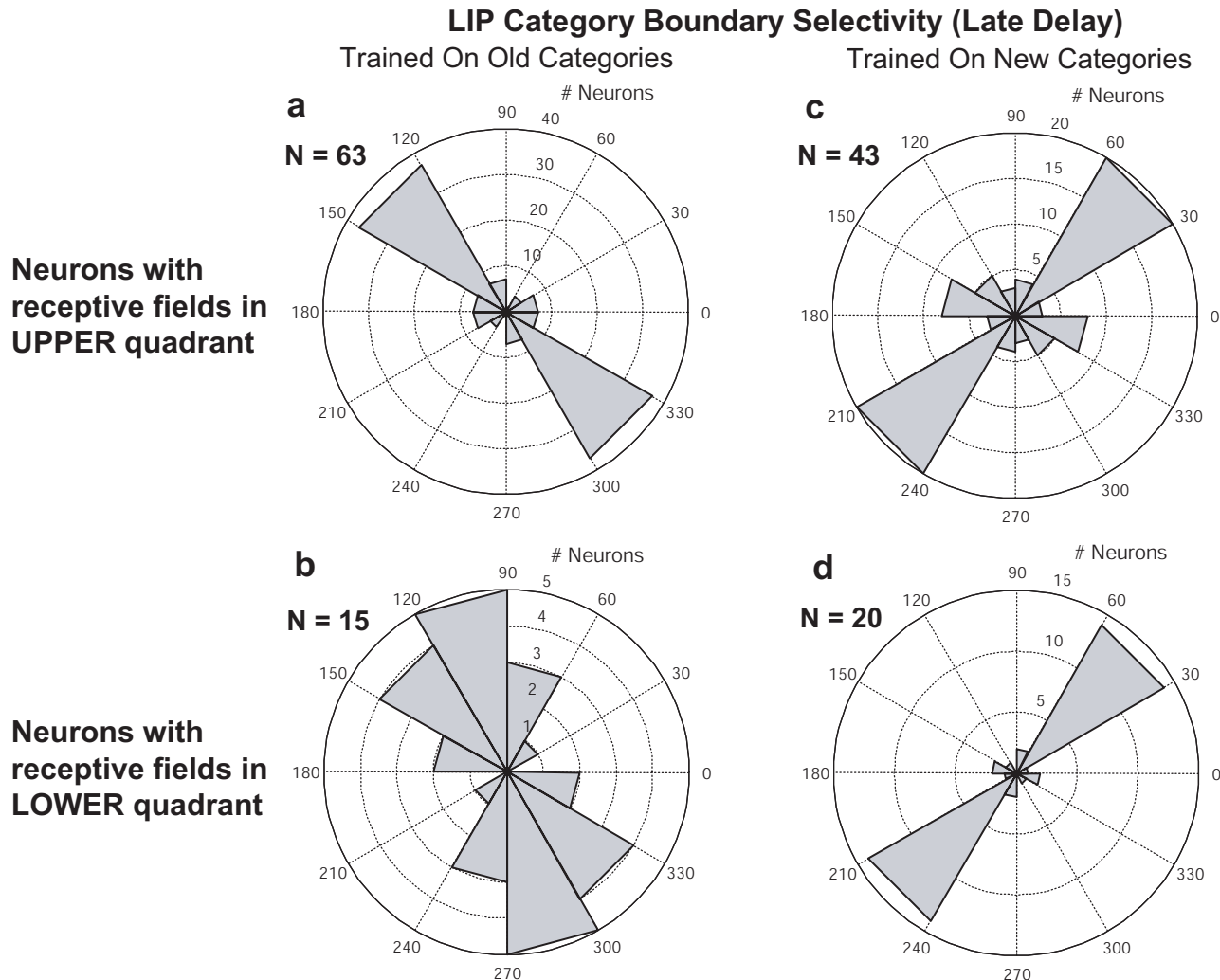
Supplementary Figure 3. MT distributions of best category boundaries. (a,b) Polar distribution of the best boundary for all MT neurons' sample (c) and delay (d) epoch activity with monkeys trained on the original category boundary (from both monkeys, $N = 67$). Each of the six possible category boundaries is represented by the six "bowtie" shapes (pairs of opposite wedge segments) on the polar histogram. The total number of neurons that prefer each boundary corresponds to the radius of either of the two opposite segments of the bowtie (but the two should not be added together).



Supplementary Figure 4. Error Trial Analysis. LIP category selectivity was stronger on correct than error trials, suggesting a link between LIP activity and categorization-task performance. For each neuron, we computed the ROC area between firing rates to preferred and non-preferred stimuli on both correct and error trials. This analysis returned values between 0.0 and 1.0, where values greater than 0.5 indicate stronger responses for the preferred category. Values less than 0.5 indicate stronger responses to the non-preferred category. This analysis revealed that category selectivity (ROC area) among direction selective neurons was significantly stronger on correct trials (sample: mean ROC area = 0.64; delay: mean ROC area = 0.70) vs. error trials (sample: mean ROC area = 0.44; delay: mean ROC area = 0.46) according to a paired t-test (sample: $p = 10^{-12}$; delay: $p = 10^{-9}$).

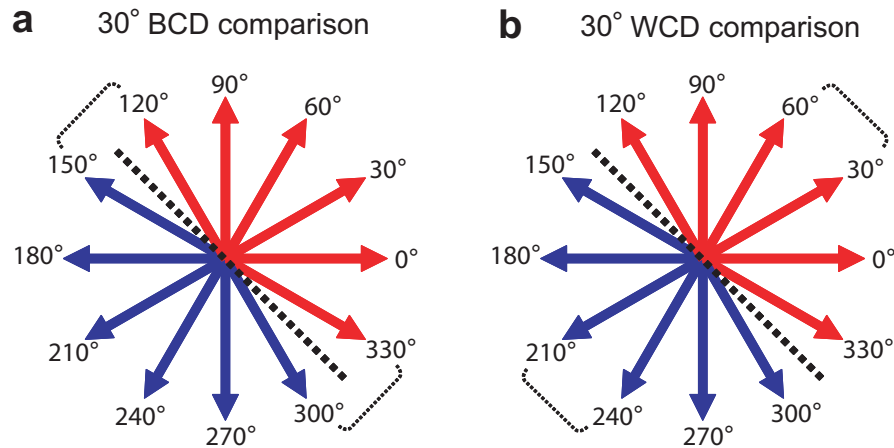


Supplementary Figure 5. Test Epoch Category Selectivity (a) The strength of category-tuning index values for the test stimulus during the test epoch (75 – 300 ms following test stimulus onset). The light grey bars show the distribution of category tuning index values across all neurons ($N = 156$, mean index value = 0.091, t-test, $p = 10^{-5}$), while the dark grey bars show index values across neurons that were direction-selective (for the test stimulus) during the test epoch ($N = 102/156$ neurons or 65%, mean index value = 0.138, t-test, $p = 10^{-6}$). (b) A comparison of the strength of category selectivity for the sample stimulus (during the sample epoch) and test stimulus (during the test epoch) across the entire population of neurons ($N = 156$). The abscissa shows the value of the category-tuning index for the sample stimulus during the sample epoch (75 – 300 ms following sample stimulus onset). The ordinate shows the category-tuning index value for the test stimulus computed during the test epoch (75 – 300 ms following test stimulus onset). Values of the sample and test category-tuning index showed a significant correlation coefficient of 0.47 ($P = 10^{-10}$). A majority of neurons ($N = 125/156$ or 80%) showed the same category preference for both the sample and test stimuli. Neurons with average firing rates that showed the same category preference during both the sample and test are represented by filled circles. Neurons that had a different preferred category during the sample and test epochs are shown with open circles.



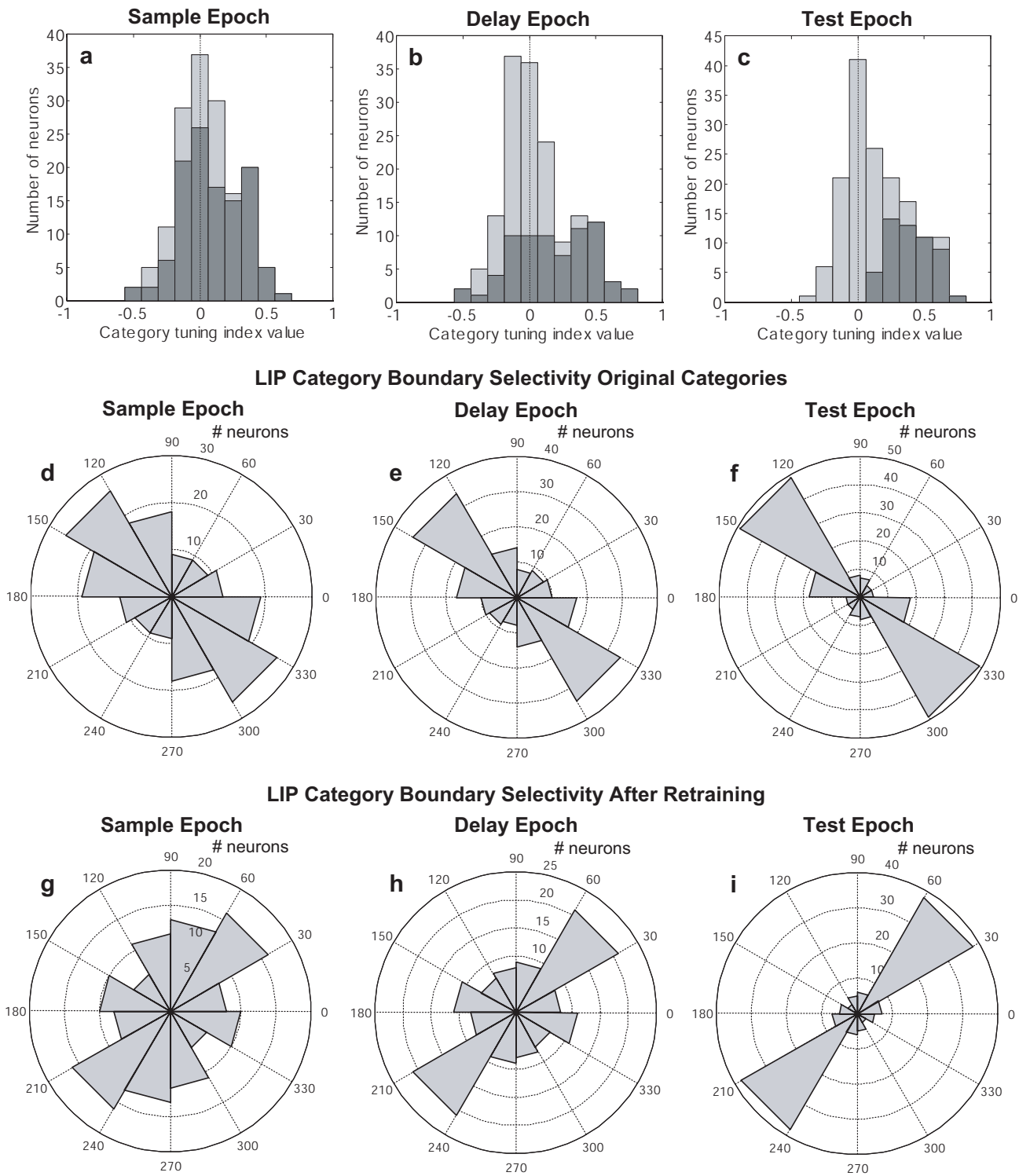
Supplementary Figure 6. There was no obvious relationship between LIP category selectivity and receptive field location. We recomputed the best boundary analysis (shown in figure 4) separately for the populations of LIP neurons with receptive field locations in the upper and lower quadrants of the visual field (relative to fixation). For each neuron, we determined which of the six possible category boundaries (i.e., the “new” and “old” boundaries, plus the four other boundaries that we did not use) gave the largest difference in average firing rate across directions on either side of the boundary. **(a,b)** Polar distributions of the best boundary during the late delay epoch with monkeys trained on the original category boundary, separated according to the location of LIP receptive fields (a: upper quadrant; b: lower quadrant). Each of the six possible category boundaries is represented by the six “bowtie” shapes (pairs of opposite wedge segments) on the polar histogram. The total number of neurons that prefer each boundary corresponds to the radius of either of the two opposite segments of the bowtie (but the two should not be added together). **(c,d)** Polar distributions of the best boundary during the late delay epoch with monkeys trained on the new category boundary, separated according to the location of LIP receptive fields (c: upper quadrant; d: lower quadrant).

Supplementary Figure 7



Supplementary Figure 7. Example of 30° BCD and WCD calculations. (a) The 30° BCD value was computed across the two pairs of directions that were 30° apart and crossed the category boundary (e.g., 120° - 150° and 300° - 330°). (b) The 30° WCD value was computed across the two pairs of directions that crossed a line perpendicular to the category boundary (e.g., 210° - 240° and 30° - 60°). This process was repeated for the other four direction intervals (60°, 90°, 120°, and 150°) giving average BCD and WCD values for each of the five intervals. These five average values were in turn averaged, giving one BCD and one WCD value for each neuron.

Supplementary Figure 8



Supplementary Figure 8. Category selectivity analyses in sample, delay and test epochs.

Category-tuning index and best-boundary analyses are shown using three time windows (rather than the two time epochs used in the main text) that are aligned to the phases of the task. The sample epoch is the same as in the original manuscript. The delay epoch is 900 ms long, beginning 100 ms following offset of the sample stimulus. The test epoch is a 300 ms window beginning at the time of test stimulus onset. Panels a-c show the values of the category index analysis in each of these three time epochs. Panels d-f show the category-boundary analysis in each of these three epochs for the data collected with the original category boundary. Panels g-i show the category-boundary analysis in each of the three epochs for the data collected after both monkeys were retrained with the new category boundary.